



Higher-order spectral filtering effects on the dynamics of stationary soliton in dissipative systems in the presence of linear and nonlinear gain/loss

Gaétan Kuetche Saadeu · Laurent Nana 

Received: 19 May 2021 / Accepted: 5 July 2021 / Published online: 26 July 2021
© The Author(s), under exclusive licence to Springer Nature B.V. 2021

Abstract In the present work, the influence of self-steepening (SS), self-frequency shift (SFS) and delayed Raman scattering (DRS) on the dynamics of solitons in a dissipative system in the presence of spectral filtering and nonlinear gain is investigated analytically and numerically in the framework of the Complex Cubic-Quintic Ginzburg-Landau Equation (CCQGLE). In this regards, a variation method is applied to obtain a dynamical model with finite degrees of freedom for the description of stationary solutions. The numerical results showed that, a weak change in value of the parameters describing the bifurcation terms leads to a qualitatively different behavior in the evolution of the pulse solutions. We have shown that the strong dependence of the momentum dynamics on the parameters describing the terms is related to the existence of a Poincaré-Andronov-Hopf bifurcation and the appearance of the unstable limit cycle. The bifurcation analysis of the dynamical system reveals the existence of fixed points which can be centers, saddles, sinks and sources. A phenomenon of nonlinear stability has been investigated and it has been shown that long living pulsating solutions with relatively small fluctuations of amplitude and frequencies exist at the bifurcation point. We have also shown that nonlinear gradient terms and

higher-order dispersion terms can change the shape and direction of propagation of the structure. We got the cases where the structure was gaining energy and the cases where it was losing energy. All our theoretical predictions have been confirmed by the direct numerical solution of the full perturbed CCQGLE. The comparison between the results obtained by the dynamical model and the direct numerical solution of the perturbed CCQGLE has proved the applicability of the proposed model in the study of the solutions of the perturbed CCQGLE.

Keywords Nonlinear gradient terms · Higher-order dispersion · Complex Cubic-Quintic Ginzburg-Landau Equation · Poincaré-Andronov-Hopf bifurcation · Soliton · Nonlinear stability

1 Introduction

It is commonly observed shapes and structures whose patterns are periodically repeated in space. These structures can naturally develop on the coat of a tiger or a giraffe, on a fingerprint, on the surface of a chemical solution, or even in the hexagonal form of cells inside the beehive. Also in optics, the spatial self-organization of light is sometimes witnessed. All these phenomena find their originality and their motivation in the capacity which these systems have to display order whereas their complexity would tend rather towards chaotic states

G. Kuetche Saadeu · L. Nana (✉)
Pure Physics Laboratory, Group of Nonlinear phenomena
in Complex Systems, Department of Physics, Faculty of
Sciences, University of Douala, P.O. Box 24157, Douala,
Cameroon
e-mail: la_nanad@yahoo.fr

[1]. This capacity is known as the principle of morphogenesis.

The “soliton” concept was first discovered by an engineer named John Scott Russell in 1834 [2]. The optical soliton on the other hand was theoretically discovered by Hasegawa and Tappert in 1973 [3], then his experimental observation in 1980 was demonstrated by Mollenauer et al. [4]. The soliton or the solitary wave which is a physical phenomenon appearing in the nonlinear and dispersive environments is defined as a localized disturbance which can propagate without deformation over long distances, and losing none of its characteristics neither by damping, nor by effect of possible shock with a disturbance of the same nature. This is why the optical soliton transmission technique is an attractive alternative for optimizing performance and eliminating propagation losses. The possibility of generating soliton structures in nonlinear media is of considerable interest due to potential applications in all-optical information processing and transport. In telecommunication, temporal solitons are carriers in dispersion compensated optical fiber transmission systems [5]. Bright temporal soliton is generated compensating anomalous group dispersion by cubic (Kerr) nonlinearity. Such a few-parameters family of solitons is well described by $(1 + 1)$ -dimensional nonlinear Schrödinger equation; one transverse dimension corresponds to the time and the propagation coordinate is the space [6]. A prerequisite to establish a bridge between the theory and the experiment is to consider real systems that are generally dissipative. In such systems, the soliton structure can be preserved if appropriate gains match linear and nonlinear losses [7]. In order to stabilize this dissipative soliton the saturating nonlinearity containing also a quintic term of opposite signs is required. As a consequence, the few-parameters family of solutions is reduced to a one fixed solution for a given set of dissipative parameters.

Indeed, the propagation of a high intensity light pulse in an optical fiber can generate a large number of nonlinear effects including stimulated Brillouin scattering (SBS), stimulated Raman scattering (SRS) and optical Kerr effects. The optical Kerr effect, which is essentially a change in the refractive index depending on the optical power, leads to many side effects, such as auto-phase modulation (SPM) and phase intermodulation (XPM), four-wave mixing (FWM) or modulation instability (MI) [8]. These different nonlinear effects greatly complicate the use of fiber, but on the

other hand they are at the origin of several interesting applications, such as all-optical regeneration, wavelength conversion, super generation continuum [8,9], to cite few. However, the use of nonlinear fiber optic devices has revolutionized communication systems and the needs in this area are likely to increase significantly in the near future.

Recently, it has been shown that passive mode-locked laser systems are described by Complex Cubic-Quintic Ginzburg-Landau Equation (CCQGLE) and Complex Cubic-Quintic Swift-Hohenberg Equation (CCQSHE) [10]. Other optical systems are also modeled by these model equations, such as transverse soliton effects in large aperture lasers and pulse propagation in optical fibers with linear (or nonlinear) gain and spectral filtering [11]. In a more recent work, the authors explore the transitions of solutions in the CCQGLE in the presence of nonlinear gain, nonlinear gain saturation, and higher-order effects such as self-steepening, third-order dispersion, and intra-pulse Raman scattering in the anomalous dispersion region [6]. Two methods (of variation and of moments) are applied to obtain the dynamical models with finite degree of freedom for the description of pulsating and stationary solutions. After applying the first model and its bifurcation analysis, the authors discovered the existence of families of subcritical Poincaré-Andronov-Hopf bifurcations due to intrapulse Raman scattering and nonlinear gains. They also studied a nonlinear stability phenomenon and showed that long-lived pulsed solutions with relatively small amplitude and frequency fluctuations exist at the bifurcation point. Wang et al. studied the propagation of optical solitons under the influence of dispersion terms in a lossy fiber system [12]. The authors show that the amplification of optical solitons can be achieved by choosing different values of the third-order dispersion. Moreover, the interactions between solitons can be reduced by setting an appropriate value of the group velocity dispersion. Gurevich et al. studied the dynamics of a single soliton solution under the influence of higher-order nonlinear and dispersive effects in the CCQGLE model [13]. The authors show how the splitting of the explosion modes is affected by the interaction of higher-order effects, resulting in the controllable selection of periodic explosions on the right or left side. In addition, they show that higher-order effects induce a series of pulsed instabilities, significantly reducing the stability region of the single soliton solution. Chen et al. used the higher-order

nonlinear Schrödinger equation to study the periodic interactions of solitons for use in optical fibers [14]. The authors analyze the interactions between the nonlinearity and the corresponding dispersion.

In the present work, we focus our interest on the major problem which takes place in the single mode optical fibers during the propagation of a signal. This major problem concerns the phenomenon of dispersion and the problem of the disturbance of solitons during the propagation in a single mode optical fiber, thus causing losses. For this purpose, we opted to study by modeled the propagation of soliton in a nonlinear dispersive medium. The aforementioned modeling led us to a nonlinear partial differential equation known in optics as the nonlinear CCQGLE, which requires digital resolution. In this regards, the present work is achieved by investigating a CCQGLE, which is widely used to describe various dissipative systems in effect of the nonlinear gradient term [18]. Our main motivation is looking at the effects of the fourth-order linear dispersion which is an explosion term and we believe that by combining it with the nonlinear gradient terms which stabilize the system we can make the soliton propagates over a long distance. And Except for a some particular sets of parameters, there are no exact analytical solutions of CCQGLE [15]. Such complex systems are treated mainly numerically. However, in order to have a better physical insight into the problem, an analytical approach even though approximate is needed. This led us to extend the variation approach to the CGLE [6]. Based on this variational approach, an analytical stability criterion for steady state solutions of CGLE has been obtained. Consequently, if such stable solutions are taken as input for direct numerical simulations, they evolve into solitons. We demonstrate that numerical solution always leads to stable dissipative one-dimensional solitons.

The paper is organized as follows. The physical meaning of the perturbation terms and applications of the generalized CCQGLE are presented in Sect. 2. In Sect. 3, we reduce the CCQGLE to a system of four first-order ordinary differential equations (ODE's) and examine its properties. Section 4 is devoted to the numerical analysis of the dynamical system. In Sect. 5, we present the results of direct numerical simulations of the basic equation by the finite difference method and we compare these results with the results of the analysis of the dynamical model. The influence of perturbation parameters on soliton dynamics is discussed

in Sect. 6, under an energetic approach. Finally, Sect. 7 concludes the study.

2 Basic equation

The dynamic behavior is described by the following CCQGLE perturbed by higher-order nonlinear and dispersive effects (*HOE's*) [6, 12–14, 17, 18]:

$$\begin{aligned} i \frac{\partial E}{\partial z} + \frac{D}{2} \frac{\partial^2 E}{\partial t^2} + s|E|^2 E \\ = i\delta E + i\beta \frac{\partial^2 E}{\partial t^2} + i\varepsilon|E|^2 E \\ - \nu|E|^4 E + i\mu|E|^4 E + HOE, \end{aligned} \quad (1)$$

where E is the normalized complex field with two independent variables, i.e. $E = E(z, t)$. The physical meaning of each particular term depends on the dynamical system under consideration. For example, in the mode-locked laser system $E(z, t)$ is the normalized amplitude of the electric field, t and z represent the evolutionary and spatial variables. Here, z is the normalized propagation distance and t is the retarded time (or the normalized transverse spatial coordinate). Thus, the variable t can take positive or negative values. Equation (1) is then the normalized form of the CCQGLE. In Eq. (1), the term $i\beta \frac{\partial^2 E}{\partial t^2}$ in the time domain clearly corresponds to $-(\omega - \omega_0)^2 E$ in the frequency domain, where ω is the frequency and ω_0 is the center frequency of the gain band. With β (if positive) the second-order spectral filtering coefficient (or gain dispersion). The fourth-order correction $|E|^4 E$ to second-order Kerr nonlinearity $|E|^2 E$ means that characteristics such as saturation of the nonlinearity can be modeled. The parameters D and s may only take the values ± 1 , $D = -1$ if the dispersion is normal and $D = 1$ if the dispersion is anomalous and $s = 1$ or $s = -1$ for positive or negative Kerr effect, respectively. We will restrict our analysis to the case $D = 1$ and $s = 1$, such that the left-hand side of Eq. (1) becomes the focusing nonlinear Schrödinger equation (NSE). $\delta < 0$ is the linear loss-gain coefficient, $\mu < 0$ represents the saturation of the nonlinear gain, $\nu < 0$ corresponds to the saturation of the nonlinear refractive index and ε is the nonlinear gain parameter or absorption coefficient. While the classical complex cubic-quintic GLE describes a supercritical bifurcation, in the case of subcritical instability this equation is augmented with a fifth-order terms to

allow the existence of stable pulse-like localized solutions if $\delta < 0$ and $\varepsilon > 0$. The *HOE* contributions are given by the third- and fourth-orders dispersion and the nonlinear gradient terms:

$$HOE = i\beta_3 \frac{\partial^3 E}{\partial t^3} - \beta_4 \frac{\partial^4 E}{\partial t^4} - q_2 |E|^2 \frac{\partial E}{\partial t} - q_3 E \frac{\partial |E|^2}{\partial t} - q_4 E^2 \frac{\partial E^*}{\partial t}, \quad (2)$$

where β_3 and β_4 account for the third-order dispersion (TOD) and the fourth-order dispersion (FOD), respectively, whereas the last three terms represent the nonlinear gradient terms. In fact, the parameters q_2 , q_3 and q_4 are complex constants (*i.e.* $q_k = q_{kr} + iq_{ki}$, $k = 2, 3, 4$) related, respectively, to the effect of self-steepening, delayed Raman scattering and self-frequency shift, representing the nonlinear gradient terms which have the role of establishing the equilibrium between the nonlinear and the dispersion terms. The four last terms of Eq. (2) are of major significance for the present study. The effect of nonlinear gradient terms on pulsating, erupting and creeping solitons of CCQGLE have been analyzed by numerical method [19]. It was shown that the nonlinear gradient terms result in dramatic changes in the soliton behavior. However, in our knowledge, the bifurcation analysis and the effects of the nonlinear gradient terms on the evolution of the soliton propagating in the CCQGLE have not been previously studied, which will be pursued in the present work.

Equation (1) has been used to model the linear wave growth problem in soliton transmission systems, amplified with limited bandwidth [20]. In optics, this equation describes laser systems [21], soliton transmission lines with regeneration [22], nonlinear cavities with an external pump [23]. This equation has been proposed as the master equation for additive pulse mode-locking in solid-state laser theory [24]. It has proven to be a good model for real mode-locked lasers, although it is basically a phenomenological model [25]. Equation (1) finds application in modeling, for example, a large aperture, short pulse optical cavity. The gain and loss of the pulse in the cavity are due to dissipative terms. The nonlinear transmission characteristics in the optical cavity are due to higher-order dissipative terms that allow, for

example, passive mode locking [26]. The phase self-modulation of light in a dispersive medium (e.g., an optical fiber) is another application of Eq. (1) [27]. This equation is a natural extension of the one-dimensional CGLE.

Several approaches have been used for the analysis of Eq. (1). The first one consisted in finding analytically the stationary solutions of the CGLE [28]. Unfortunately, only the cubic CGLE could be fully analyzed in this way. Although a large variety of impulsive and stationary solutions of the cubic CGLE were found, these solutions exist only in a subspace of the lower dimensional parameter space. Furthermore, these solutions are unstable except for trivial solution impulses and flat-top impulses. The second approach is based on approximate methods such as perturbation theory (PT) [29]. In particular, the PT applied to the soliton of the Schrödinger equation can be developed around the solution. In this case, the PT predicts the existence of two stationary solutions, one of them being stable and the other unstable. However, the PT only applies if the dissipative terms are small. Finally, one can solve numerically Eq. (1), which has been done in several papers [5, 6, 12, 14, 17].

3 Reduction to the ODE set and bifurcation analysis

One of the ways to find stationary solutions of Eq. (1) consists in its reduction to a set of ordinary differential equations (ODE's). We seek the soliton solution in the form:

$$E(z, t) = \eta(z) \operatorname{sech}\{\eta(z)[t - k(z)]\} e^{\{-i\omega(z)[t - k(z)] + i\alpha(z)\}}, \quad (3)$$

where $\eta(z)$ is the amplitude, $\omega(z)$ is the frequency, $k(z)$ is the position of the pulse soliton and $\alpha(z)$ is the phase. By applying the perturbation theory by means of Lagrangian approach [5, 6], we obtain a system of ODE's which describes the evolution of soliton parameters in the presence of all ten perturbation terms in the right hand side of Eq. (1):

$$\left\{ \begin{aligned} \frac{\partial \eta}{\partial z} &= 2\delta\eta + \frac{4}{3}(q_{2r} - q_{4r})\eta^3\omega + \frac{2}{3}(2\varepsilon - \beta)\eta^3 \\ &\quad + \frac{16}{15}\mu\eta^5 - 2\beta\eta\omega^2, \\ \frac{\partial \omega}{\partial z} &= \frac{4}{15}(q_{2r} + 2q_{3r} + q_{4r})\eta^4 - \frac{4}{3}\beta\eta^2\omega, \\ \frac{\partial k}{\partial z} &= -\omega + \frac{1}{3}(3\beta_3 + q_{2i} + 2q_{3i} + q_{4i})\eta^2 \\ &\quad + 4\beta_4\eta^2\omega + 4\beta_4\omega^3 + 3\beta_3\omega^2, \\ \frac{\partial \alpha}{\partial z} &= \frac{1}{2}(\eta^2 + \omega^2) + 2\eta^2\beta_4\omega^2 + \frac{1}{9}(21\beta_4 + 8\nu)\eta^4 \\ &\quad + \frac{2}{3}(q_{2i} + 2q_{3i} + q_{4i} + 3\beta_3)\eta^4 \\ &\quad - 3\beta_4\omega^4 - 2\beta_3\omega^3. \end{aligned} \right. \tag{4}$$

The case where $q_{2r} = q_{4r} = q_{2i} = q_{3i} = q_{4i} = \beta_4 = s = 0, q_{3r} = -\gamma$, has been studied in [6]. The first two equations of the system (4) are coupled and must be used to determine the fixed points.

$$\left\{ \begin{aligned} \frac{\partial \eta}{\partial z} &= 2\delta\eta + \frac{4}{3}(q_{2r} - q_{4r})\eta^3\omega + \frac{2}{3}(2\varepsilon - \beta)\eta^3 \\ &\quad + \frac{16}{15}\mu\eta^5 - 2\beta\eta\omega^2, \\ \frac{\partial \omega}{\partial z} &= \frac{4}{15}(q_{2r} + 2q_{3r} + q_{4r})\eta^4 - \frac{4}{3}\beta\eta^2\omega. \end{aligned} \right. \tag{5}$$

These fixed points $(\eta_{0,i}, \omega_{0,i})$ are obtained by posing:

$$\left\{ \begin{aligned} 2\delta\eta + \frac{4}{3}(q_{2r} - q_{4r})\eta^3\omega + \frac{2}{3}(2\varepsilon - \beta)\eta^3 \\ + \frac{16}{15}\mu\eta^5 - 2\beta\eta\omega^2 &= 0, \\ \frac{4}{15}(q_{2r} + 2q_{3r} + q_{4r})\eta^4 - \frac{4}{3}\beta\eta^2\omega &= 0. \end{aligned} \right. \tag{6}$$

The resolution of the system (6) by taking the amplitude of the positive solution ($\eta > 0$), gives us:

$$(\eta_{0,i}, \omega_{0,i}) = (\eta_{0,i}, \frac{q_{2r} + 2q_{3r} + q_{4r}}{5\beta}\eta_{0,i}^2), i = 1, 2, 7)$$

where $\eta_{0,1} = \sqrt{A + \sqrt{A^2 - B}}, \eta_{0,2} = \sqrt{A - \sqrt{A^2 - B}}$

with,

$$A = \frac{25\beta(\beta - 2\varepsilon)}{2C}, B = \frac{75\delta\beta}{C}$$

and

$$C = 40\beta\mu + 7q_{2r}^2 + 8q_{2r}q_{3r} - 6q_{2r}q_{4r} - 32q_{4r}q_{3r} - 12q_{3r}^2 - 13q_{4r}^2.$$

According to the values of A and B, there are:

- two steady-state solutions of amplitudes $\eta_{0,1} = \sqrt{A + \sqrt{A^2 - B}}$ and $\eta_{0,2} = \sqrt{A - \sqrt{A^2 - B}}$ if (i) $A > \sqrt{B} > 0$,
- one steady-state solution of amplitude $\eta_{0,1} = \sqrt{A + \sqrt{A^2 - B}}$ if (ii) $B < 0$,
- one steady-state solution of amplitude $\eta_{0,1} = \eta_{0,2} = \sqrt{A}$ if (iii) $A = \sqrt{B} > 0$,
- one steady-state solution of amplitude $\eta_{0,1} = \sqrt{2A}$ if (iv) $B = 0, A > 0$.

Knowing however that if $\delta < 0, \beta > 0, \mu < 0$, cases (ii) and (iv) are excluded because of the instability of the background which could be avoided if there are stable localized solutions [28]. To avoid the case (ii), we choose q_{2r} and q_{4r} in order to have $B > 0$. In addition, case (iii) is excluded because in our approach, we write one of the bifurcation parameters as a function of the others. Finally, we work with case (i).

Having the fixed points, we obtain the stationary solutions from the last two equations of the system (4).

$$\left\{ \begin{aligned} -\omega_{0,i} + \frac{1}{3}(3\beta_3 + q_{2i} + 2q_{3i} + q_{4i})\eta_{0,i}^2 \\ + 4\beta_4\eta_{0,i}^2\omega_{0,i} + 4\beta_4\omega_{0,i}^3 + 3\beta_3\omega_{0,i}^2 &= 0, \\ \frac{1}{2}(\eta_{0,i}^2 + \omega_{0,i}^2) + \frac{1}{9}(21\beta_4 + 8\nu)\eta_{0,i}^4 - 2\beta_3\omega_{0,i}^3 \\ + \frac{2}{3}(q_{2i} + 2q_{3i} + q_{4i} + 3\beta_3)\eta_{0,i}^4 \\ + 2\eta_{0,i}^2\beta_4\omega_{0,i}^2 - 3\beta_4\omega_{0,i}^4 &= 0. \end{aligned} \right. \tag{8}$$

We therefore fix the values of the imaginary parts of the gradient terms (q_{2i}, q_{3i}, q_{4i}) and we determine the dispersion terms (β_3 and β_4) which make the solution stationary.

The Jacobian matrix of the system (5) is written:

$$J = \begin{bmatrix} J_{11} & J_{12} \\ J_{21} & J_{22} \end{bmatrix} \tag{9}$$

where the elements are respectively

$$\begin{aligned}
 J_{11} &= 2\delta + 4(q_{2r} - q_{4r})\eta^2\omega \\
 &\quad + 2(2\varepsilon - \beta)\eta^2 + \frac{16}{3}\mu\eta^4 - 2\beta\omega^2, \\
 J_{12} &= \frac{4}{3}(q_{2r} - q_{4r})\eta^3 - 4\beta\eta\omega, \\
 J_{21} &= \frac{16}{15}(q_{2r} + 2q_{3r} + q_{4r})\eta^3 - \frac{8}{3}\beta\eta\omega, \\
 J_{22} &= -\frac{4}{3}\eta^2\beta.
 \end{aligned}$$

The eigenvalues of fixed point matrix are calculated by canceling the characteristic polynomial:

$$P_{J_0} = \lambda^2 - (\text{tr} J_0)\lambda + \det J_0 = 0. \tag{10}$$

Let us take the case where the eigenvalues are complex conjugate numbers (Bifurcation of Poincaré-Andronov-Hopf) and write them in the form:

$$\lambda_{1,2} = \frac{\text{tr} J_0 \pm \sqrt{\Delta}}{2} = \text{Re}(\chi) \pm i \text{Im}(\chi), \tag{11}$$

where $\Delta = \Delta(\chi) = (\text{tr} J_0)^2 - 4\det J_0$,

$$\begin{aligned}
 \text{tr} J_0 &= \frac{-2}{75\beta} [(-200\beta\mu - 27q_{2r}^2 - 48q_{2r}q_{3r} \\
 &\quad + 6q_{2r}q_{4r} + 12q_{3r}^2 + 72q_{3r}q_{4r} + 33q_{4r}^2)\eta_{0,i}^4 \\
 &\quad + (125\beta^2 - 150\beta\varepsilon)\eta_{0,i}^2 - 75\beta\delta]
 \end{aligned} \tag{12}$$

and

$$\begin{aligned}
 \det J_0 &= \frac{8\eta_{0,i}^2}{3} \left[-\beta\delta + \beta(\beta - 2\varepsilon)\eta_{0,i}^2 \right. \\
 &\quad + \left(-\frac{7}{15}q_{2r}^2 - \frac{8}{15}q_{3r}q_{2r} + \frac{2}{5}q_{2r}q_{4r} - \frac{8}{3}\beta\mu \right. \\
 &\quad \left. \left. + \frac{32}{15}q_{3r}q_{4r} + \frac{13}{15}q_{4r}^2 + \frac{4}{5}q_{3r}^2 \right) \eta_{0,i}^4 \right].
 \end{aligned} \tag{13}$$

The Poincaré-Andronov-Hopf bifurcation analysis focuses on the following results:

$$\begin{aligned}
 \text{Re}(\chi) &= \frac{1}{75\beta} [(200\beta\mu + 27q_{2r}^2 + 48q_{2r}q_{3r} \\
 &\quad - 6q_{2r}q_{4r} - 12q_{3r}^2 - 72q_{3r}q_{4r} - 33q_{4r}^2)\eta_{0,i}^4 \\
 &\quad + (-125\beta^2 + 150\beta\varepsilon)\eta_{0,i}^2 + 75\beta\delta],
 \end{aligned} \tag{14}$$

$$\text{Im}(\chi) = \frac{1}{2}\sqrt{-\Delta(\chi)}, \tag{15}$$

$$\begin{aligned}
 d &= \frac{d \text{Re}(\chi)}{d\chi} \Big|_{\chi=\chi_0}, \text{ where} \\
 \chi_0 &= \varepsilon, \mu, q_{2r}, q_{3r}, q_{4r}.
 \end{aligned} \tag{16}$$

The Poincaré-Andronov-Hopf bifurcation theory applied to the system (5) has a limit cycle (stable or unstable) when the conditions of non-hyperbolicity and transversality are enforced [31]. These conditions are:

$$\begin{aligned}
 \text{Re}(\chi_0) &= 0, \Delta(\chi_0) < 0, d \neq 0, \\
 \text{Im}(\chi_0) &= \Omega \neq 0, a \neq 0.
 \end{aligned} \tag{17}$$

The stability coefficient a is defined as in [6] by:

$$\begin{aligned}
 a &= \frac{[f_{pq}(f_{pp} + f_{qq}) - g_{pq}(g_{pp} + g_{qq}) - f_{pp}g_{pp} + f_{qq}g_{qq}]}{16\Omega} \\
 &\quad + \frac{[f_{ppp} + f_{pqq} + g_{ppq} + g_{qqq}]}{16},
 \end{aligned} \tag{18}$$

with

$$f(p, q, \chi_0) = \frac{G(p, q)}{J_{21}}, \tag{19}$$

$$g(p, q, \chi_0) = \frac{\bar{J}_{11}G(p, q) - \bar{J}_{21}F(p, q)}{\Omega \bar{J}_{21}}, \tag{20}$$

$$\begin{aligned}
 F(p, q) &= 2\delta(\bar{J}_{11}p - q\Omega + \eta_{0,i}) \\
 &\quad + \frac{4}{3}(q_{2r} - q_{4r})(\bar{J}_{11}p - q\Omega + \eta_{0,i})^3 \\
 &\quad (\bar{J}_{21}p + \omega_{0,i}) \\
 &\quad + \frac{2}{3}(2\varepsilon - \beta)(\bar{J}_{11}p - q\Omega + \eta_{0,i})^3 \\
 &\quad + \frac{16}{15}\mu(\bar{J}_{11}p - q\Omega + \eta_{0,i})^5 \\
 &\quad - 2\beta(\bar{J}_{11}p - q\Omega + \eta_{0,i}) \\
 &\quad (\bar{J}_{21}p + \omega_{0,i})^2,
 \end{aligned} \tag{21}$$

$$\begin{aligned}
 G(p, q) &= \frac{4}{15}(q_{2r} + 2q_{3r} + q_{4r}) \\
 &\quad (\bar{J}_{11}p - q\Omega + \eta_{0,i})^4 \\
 &\quad - \frac{4}{3}\beta(\bar{J}_{11}p - q\Omega + \eta_{0,i})^2 \\
 &\quad (\bar{J}_{21}p + \omega_{0,i}),
 \end{aligned} \tag{22}$$

where

$$\bar{J}_{11} = J_{11}(\chi_0), \bar{J}_{21} = J_{21}(\chi_0), \tag{23}$$

and all derivatives are calculated for the point $(p, q, \chi) = (0, 0, \chi_0)$.

The period of the limit cycle is calculated with the relation $T = \frac{2\pi}{|\Omega|}$.

The stability coefficient a and the parameter d allow us to know the type of bifurcation and to predict the evolution of the system. Two cases of bifurcations can arise, namely [31]:

Case 1: subcritical bifurcation ($a > 0$): the limit cycle is unstable

- When $d < 0$, the origin of the system has an asymptotically stable fixed point for $(\chi > \chi_0)$ and unstable for $(\chi < \chi_0)$.
- When $d > 0$, the origin of the system has an asymptotically stable fixed point for $(\chi < \chi_0)$ and unstable for $(\chi > \chi_0)$.

Case 2: supercritical bifurcation ($a < 0$): the limit cycle is stable

- When $d < 0$, the origin of the system has an asymptotically stable fixed point for $(\chi < \chi_0)$ and unstable for $(\chi > \chi_0)$.
- $d > 0$, the origin of the system has an asymptotically stable fixed point for $(\chi > \chi_0)$ and unstable for $(\chi < \chi_0)$.

Using (11), we notice the following facts:

- if $\text{tr} J_0 > 0, \det J_0 > 0$, then $\lambda_1 > 0, \lambda_2 > 0 \Rightarrow$ source,
- if $\text{tr} J_0 > 0, \det J_0 < 0$, then $\lambda_1 > 0, \lambda_2 < 0 \Rightarrow$ saddle,
- if $\text{tr} J_0 < 0, \det J_0 > 0$, then $\lambda_1 < 0, \lambda_2 < 0 \Rightarrow$ sink,
- if $\text{tr} J_0 < 0, \det J_0 < 0$, then $\lambda_1 > 0, \lambda_2 < 0 \Rightarrow$ saddle.

In this work, we obtain equations that can generate a multitude of values associated with the parameters. We fix some in order to determine the others. We can now say that the system (4) gives centers, sources, saddles and sinks if the previous conditions are respected. It remains for us to observe their phase portraits.

4 Numerical analysis of the ODE system

In this part, we analyze the system (4) in order to study the stability and bring out the analytical solution.

4.1 Bifurcation under the influence of nonlinear gain

Figure 1a shows the evolution of the frequency as a function of the amplitude for parameters calculated at the bifurcation point. We noted that the solution leaves

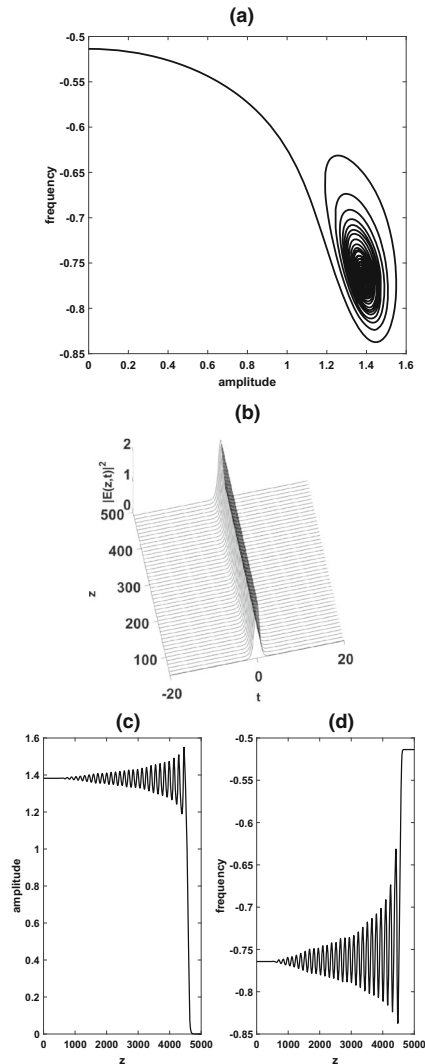


Fig. 1 Results obtained by dynamical model with parameters $\mu = -0.01, \delta = -0.02, \nu = 0.431595, A = 1.43, B = 1.82, \Delta = -0.008, d = -4.25, \beta = 0.01, \beta_3 = 0.02, \beta_4 = 0.01, q_{2i} = -0.01, q_{4i} = -0.5852, q_{3i} = -0.3, q_{2r} = 0.0101, q_{3r} = -0.0125, q_{4r} = -0.0051$. **a** Parametric plot of pulse amplitude $\eta(z)$ and frequency $\omega(z)$ for $\varepsilon = \varepsilon_0 = 0.05219006491$ (ε is equal to its bifurcation value), with initial condition $\omega_{0,1} = -0.7643127702$ and $\eta_{0,1} = 1.382310358$ for distance $z_{max} = 5000$. **b** The analytical solution which is obtained by dynamical model with the same parameters. **c, d** Spatial evolution of pulse amplitude $\eta(z)$ and frequency $\omega(z)$ with the same parameters. **e** Parametric plot of pulse amplitude $\eta(z)$ and frequency $\omega(z)$ with $\varepsilon = 0.05119006491 < \varepsilon_0$ (below bifurcation point) for distance $z_{max} = 6000$. The initial condition $\omega_{0,1} = -0.7120988092, \eta_{0,1} = 1.334258979$. **f** Parametric plot of pulse amplitude $\eta(z)$ and frequency $\omega(z)$ with $\varepsilon = 0.05319006491 > \varepsilon_{0,1}$ for distance $z_{max} = 3000$. The initial condition $\omega_{0,1} = -0.8101418431, \eta_{0,1} = 1.423149538$

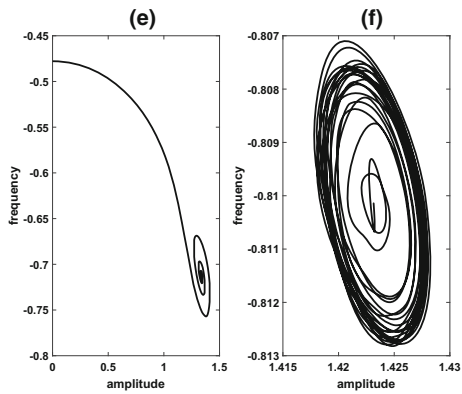


Fig. 1 continued

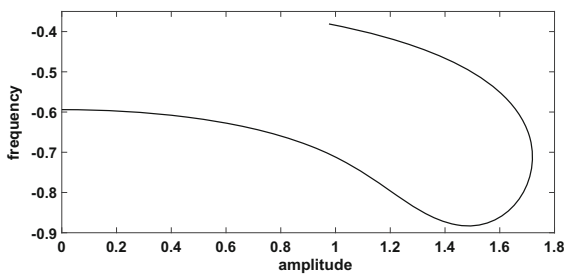


Fig. 2 Results obtained by dynamical model with parameters $\mu = -0.01, \delta = -0.02, \nu = 0.431595, A = 1.43, B = 1.82, \Delta = 0.0049, tr J_0 = 0.05374358035, det J_0 = -0.0005095377829, \beta = 0.01, \beta_3 = 0.02, \beta_4 = 0.01, q_{2i} = -0.01, q_{4i} = -0.5852, q_{3i} = -0.3, q_{2r} = 0.0101, q_{3r} = -0.0125, q_{4r} = -0.0051$. Parametric plot of pulse amplitude $\eta(z)$ and frequency $\omega(z)$ for $\varepsilon = \varepsilon_0 = 0.05219006491$ (ε is equal to its bifurcation value), with initial condition $\omega_{0,2} = -0.3810771550$ and $\eta_{0,2} = 0.9760598791$ for distance $z_{max} = 5000$.

the fixed point to go to form the unstable limiting cycle ($a = 0.000767002 > 0$) whose period is $T = 138.78$. Figure 1b is the analytical solution which is obtained with the same values of parameters. Figure 1c, d shows the frequency oscillation and the amplitude around the average values $\omega_m = \omega_{0,1}$ and $\eta_m = \eta_{0,1}$. The study around the bifurcation is given to us by Fig. 1e, f. These curves show that the origin of the system has an unstable fixed point for $\varepsilon < \varepsilon_0, T = 168.70$ and asymptotically stable for $\varepsilon > \varepsilon_0, T = 121.13$. These results are predictable because by calculation, we obtained $d < 0$.

Figure 2 shows the evolution of the frequency as a function of the amplitude for the second fixed point $(\eta_{0,2}, \omega_{0,2})$. The chosen parameters allow us to have the sign of the eigenvalues ($\lambda_1 > 0, \lambda_2 > 0$). We can therefore say that the fixed point is an unstable saddle.

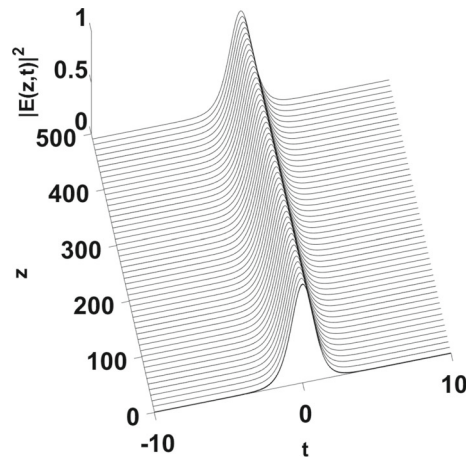
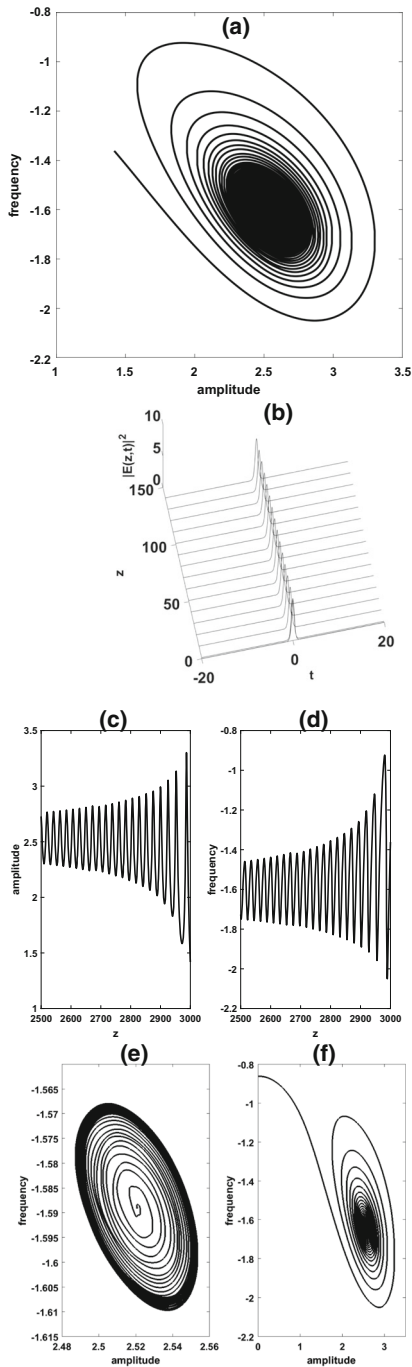


Fig. 3 Results obtained by dynamical model with parameters $\mu = -0.01, \delta = -0.02, \nu = 0.431595, A = 1.43, B = 1.82, \Delta = 0.0049, tr J_0 = 0.05374358035, det J_0 = -0.0005095377829, \beta = 0.01, \beta_3 = 0.02, \beta_4 = 0.01, q_{2i} = -0.01, q_{4i} = -0.5852, q_{3i} = -0.3, q_{2r} = 0.0101, q_{3r} = -0.0125, q_{4r} = -0.0051, \varepsilon = \varepsilon_0 = 0.05219006491, \omega_{0,2} = -0.3810771550, \eta_{0,2} = 0.9760598791, z_{max} = 5000$.

Figure 3 shows that it is also possible to obtain a stationary soliton with the second fixed point while remaining under the conditions of Eq. (8). The cubic term therefore allows us to control the nonlinear gain.

4.2 Bifurcation under the influence of the saturation of nonlinear gain

Figure 4a shows the evolution of the frequency as a function of the amplitude for parameters calculated at the bifurcation point. We note that the solution leaves the fixed point to go to form an unstable limit cycle ($a = 0.009642260929 > 0$) whose period is $T = 20.80$. Figure 4b is the analytical solution which is obtained with the same values of parameters. Figure 4c, d shows frequency oscillation and amplitude around mean values $\omega_m = \omega_{0,1}$ and $\eta_m = \eta_{0,1}$. The study around the bifurcation is given to us by Fig. 4e, f. These curves show that the origin of the system has an asymptotically stable fixed point for $\mu < \mu_0, T = 21.20$ and unstable for $\mu > \mu_0, T = 20.40$. These results are predictable because by calculation, we obtained $d > 0$. The quintic term saturates the nonlinear gain.



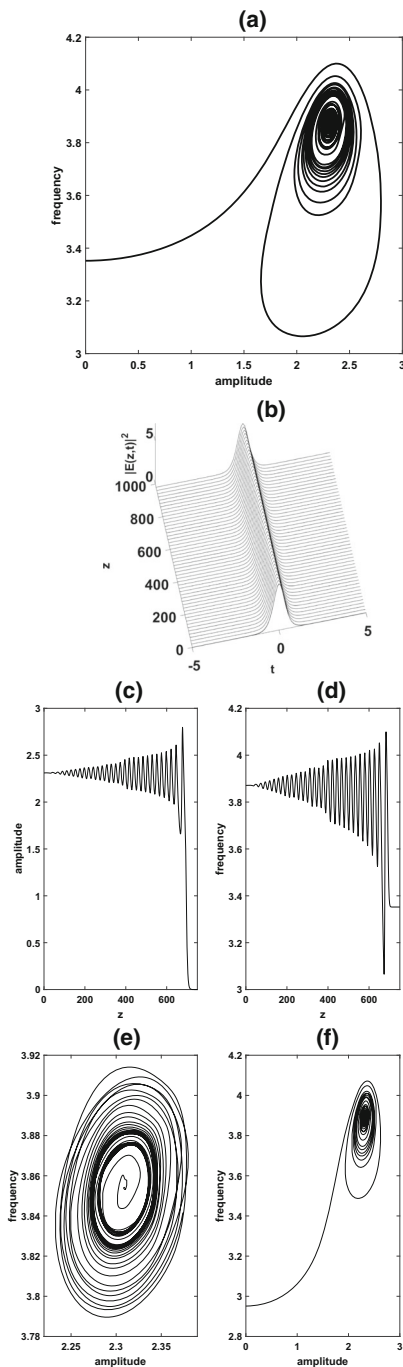
◀ **Fig. 4** Result obtained by numerical simulation of the ODE system with parameters $\varepsilon = 0.05, \delta = -0.02, \nu = 0, A = 3.65, B = 5.48, \Delta = -0.36, d = 45.59, \beta = 0.02, \beta_3 = -0.021, \beta_4 = 0, q_{2i} = q_{4i} = 0, q_{3i} = -0.3, q_{2r} = 0.0051, q_{3r} = -0.0125, q_{4r} = -0.0051$. **a** Parametric plot of pulse amplitude $\eta(z)$ and frequency $\omega(z)$ for $\mu = \mu_0 = -0.001307426986$ (μ is equal to its bifurcation value), with initial condition $\omega_{0,1} = -1.615723557$ and $\eta_{0,1} = 2.542222301$ for distance $z_{max} = 3000$. **b** The analytical solution which is obtained by dynamical model with the same parameters. **c, d** Spatial evolution of pulse amplitude $\eta(z)$ and frequency $\omega(z)$ with the same parameters. **e** Parametric plot of pulse amplitude $\eta(z)$ and frequency $\omega(z)$ with $\mu = -0.001407426986 < \mu_0$ (below bifurcation point) for distance $z_{max} = 3000$. The initial condition $\omega_{0,1} = -1.588909823, \eta_{0,1} = 2.521039328$. **f** Parametric plot of pulse amplitude $\eta(z)$ and frequency $\omega(z)$ with $\mu = -0.001207426986 > \mu_0$ for distance $z_{max} = 1000$. The initial condition $\omega_{0,1} = -1.643314673, \eta_{0,1} = 2.563836713$

4.3 Bifurcation under the influence of nonlinear gradient term

The importance of including nonlinear gradient terms in order to properly predict the post localization behavior [32]. These nonlinear gradient terms allow the stabilization of the system [18].

4.3.1 Case of self-steepening

Figure 5a represents the evolution of the frequency as a function of the amplitude for parameters calculated at the bifurcation point. We noted that the solution leaves the fixed point to go to form an unstable limit cycle ($a = 0.065806028 > 0$) whose period is $T = 21.56$. Figure 5b is the analytical solution which is obtained with the parameters satisfying Eq. (8). We note that the structure remains stable and stationary whatever the distance. Figure 5c, d shows the frequency oscillation and the amplitude around the mean values $\omega_m = \omega_{0,1}$ and $\eta_m = \eta_{0,1}$. The study around the bifurcation is given to us by Fig. 5e, f. These curves show that the origin of the system has an asymptotically stable fixed point for ($q_{2r} < q_{2r0}, T = 21.595$) and unstable for ($q_{2r} > q_{2r0}, T = 21.516$). These results were predictable because by calculation, we obtain $d > 0$.



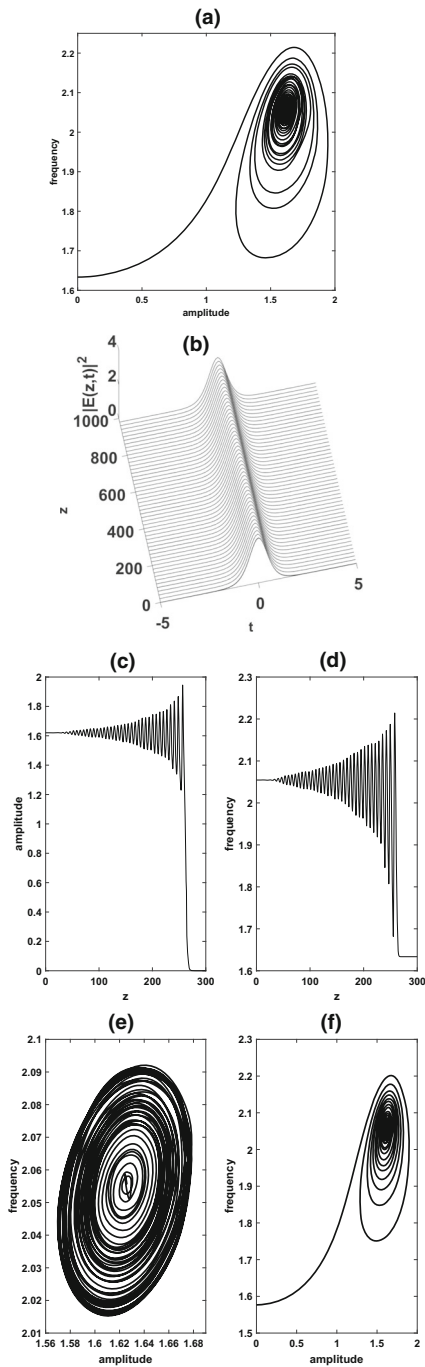
◀ **Fig. 5** Result obtained by numerical simulation of the ODE system with parameters $\varepsilon = 0.1, \nu = 0, \mu = -0.01, \delta = -0.02, A = 2.83, B = 1.79, \Delta = -0.33, d = 15.78, \beta = 0.01, \beta_3 = 0.2824603941, \beta_4 = -0.03068936474, q_{2i} = 0.2, q_{4i} = 0.02, q_{3i} = -0.3, q_{3r} = 0.02381, q_{4r} = -0.0051$. **a** Parametric plot of pulse amplitude $\eta(z)$ and frequency $\omega(z)$ for $q_{2r} = q_{2r_0} = -0.0062794$ (q_{2r} is equal to its bifurcation value), with initial condition $\omega_{0,1} = 3.871198193$ and $\eta_{0,1} = 2.310767038$ for distance $z_{max} = 800$. **b** The analytical solution which is obtained by dynamical model with the same parameters. **c, d** Spatial evolution of pulse amplitude $\eta(z)$ and frequency $\omega(z)$ with the same parameters. **e** Parametric plot of pulse amplitude $\eta(z)$ and frequency $\omega(z)$ with $q_{2r} = -0.0063794 < q_{2r_0}$ (below bifurcation point) for distance $z_{max} = 900$. The initial condition $\omega_{0,1} = 3.854061978, \eta_{0,1} = 2.30912089$. **f** Parametric plot of pulse amplitude $\eta(z)$ and frequency $\omega(z)$ with $q_{2r} = -0.0061794 > q_{2r_0}$ for distance $z_{max} = 800$. The initial condition $\omega_{0,1} = 3.888574992, \eta_{0,1} = 2.313045601$.

4.3.2 Case of delayed Raman scattering

Figure 6a represents the evolution of the frequency as a function of the amplitude for parameters calculated at the bifurcation point. We noted that the solution leaves the fixed point to go to form an unstable limit cycle ($a = 1.279628249 > 0$) whose period is $T = 6.37$. Figure 6b is the analytical solution which is obtained with the parameters satisfying Eq. (8). We note that the structure remains stable and stationary whatever the distance. Figure 6c, d shows the frequency oscillation and the amplitude around the average values $\omega_m = \omega_{0,1}$ and $\eta_m = \eta_{0,1}$. The study around the bifurcation is given to us by Fig. 6e, f. These curves show that the origin of the system has an asymptotically stable fixed point for ($q_{3r} < q_{3r_0}, T = 6.32$) and unstable for ($q_{3r} > q_{3r_0}, T = 6.42$). These results were predictable because by calculation, we obtain $d > 0$.

5 Results of direct numerical simulations

The numerical results of the solutions of Eq. (1) are obtained from the finite difference method [16]. The finite difference method consists in approximating the



◀ **Fig. 6** Results obtained by dynamical model with parameters $\varepsilon = 0.65, v = 0, \mu = -0.1, \delta = -0.1, A = 1.448, B = 0.71, \Delta = -3.888, d = 10.426, \beta = 0.08, \beta_3 = 0.8126897882, \beta_4 = -0.1735770653, q_{2i} = -0.1, q_{3i} = -0.3, q_{4i} = 0.01, q_{2r} = -0.07806, q_{4r} = -0.0051$. **a** Parametric plot of pulse amplitude $\eta(z)$ and frequency $\omega(z)$ for $q_{3r} = 0.1980793602$ (q_{3r} is equal to its bifurcation value), with initial condition $\omega_{0,1} = 2.054545076$ and $\eta_{0,1} = 1.620378797$ for distance $z_{max} = 300$. **b** The analytical solution which is obtained by dynamical model with the same parameters. **c, d** Spatial evolution of pulse amplitude $\eta(z)$ and frequency $\omega(z)$ with the same parameters. **e** Parametric plot of pulse amplitude $\eta(z)$ and frequency $\omega(z)$ with $q_{3r} = 0.1970793602 < q_{3r_0}$ (below bifurcation point) for distance $z_{max} = 400$. The initial condition $\omega_{0,1} = 2.055567522, \eta_{0,1} = 1.625985125$. **f** Parametric plot of pulse amplitude $\eta(z)$ and frequency $\omega(z)$ with $q_{3r} = 0.1990793602 > q_{3r_0}$ for distance $z_{max} = 500$. The initial condition $\omega_{0,1} = 2.053449388, \eta_{0,1} = 1.614795768$.

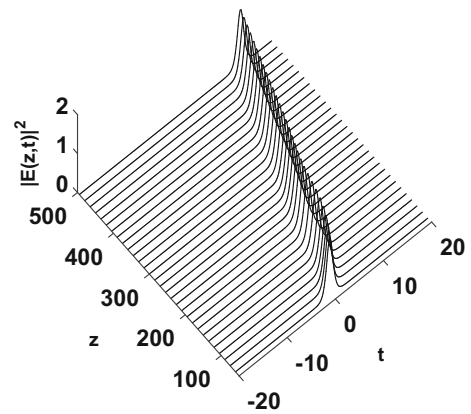


Fig. 7 Result of direct numerical simulation obtained by Eq. (1) with the parameters $\mu = -0.01, v = 0.43, \delta = -0.02, A = 1.43, B = 1.82, \Delta = -0.008, d = -4.25, \beta = 0.01, \beta_3 = 0.02, \beta_4 = 0.01, q_{2i} = -0.01, q_{4i} = -0.58527, q_{3i} = -0.3, q_{2r} = 0.0101, q_{3r} = -0.0125, q_{4r} = -0.0051, \varepsilon = \varepsilon_0 = 0.05219006491, \omega_{0,1} = -0.7643127702, \eta_{0,1} = 1.382310358$

derivatives of the equations of physics by means of Taylor expansions and is deduced directly from the definition of the derivative. Using this method, we simulate the temporal and spatial evolution of the normalized

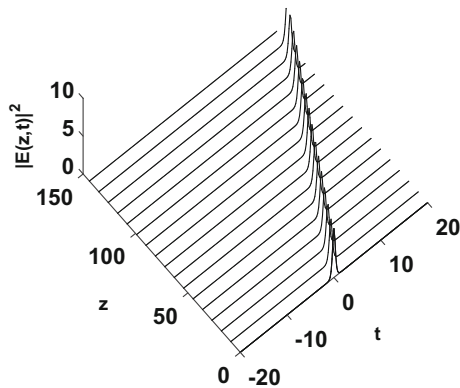


Fig. 8 Result of direct numerical simulation obtained by Eq. (1) with the parameters $\varepsilon = 0.05$, $\nu = 0$, $\delta = -0.02$, $A = 3.65$, $B = 5.48$, $\Delta = -0.36$, $d = 45.59$, $\beta = 0.02$, $\beta_3 = -0.021$, $\beta_4 = 0$, $q_{2i} = q_{4i} = 0$, $q_{3i} = -0.3$, $q_{2r} = 0.0051$, $q_{3r} = -0.0125$, $q_{4r} = -0.0051$, $\mu = \mu_0 = -0.001307426986$, $\omega_{0,1} = -1.615723557$, $\eta_{0,1} = 2.542222301$

electric field intensity profile. The simulation starts from an approximation of a pulse-like soliton [Eq. (3)] with a low amplitude. The objective of this simulation study is to analyze the effects of the different bifurcation parameters in the construction and propagation of soliton solutions. The figures above represent the temporal and spatial evolution of the intensity of the localized solution of the soliton of Eq. (1) for the regime of anomalous dispersion. There is an excellent agreement between the direct numerical solutions (Figs. 7 and 8) and the analytical solutions (Figs. 1 and 4). This confirms the applicability of our dynamical model [Eq.(4)]. It is largely clear that the soliton retains its shape and direction during its spatial propagation. It should be noted that the character of the intensity is invariant during propagation and the temporal width of the pulse soliton remains stable during this propagation. By modifying the effects of dispersion and nonlinearity, the soliton moves in this medium without deforming (oscillating around an average value) [7].

6 Discussion

In the above analysis, we have found soliton solutions of the CCQGLE for the case of anomalous dispersion (i.e. $D = 1$). The solutions have been obtained numerically as a function of the parameters of the system, after

application of an appropriate perturbation theory. The bifurcation analysis of the dynamical system revealed that the fixed point can be a center, a saddle, a sink and a source. The structure thus created propagates by oscillating around its fixed points. Very short impulse-type solitons whose duration is of the order of femto seconds $10^{-15}s$ have a very broad spectrum and correspond to the significant contributions of the dispersion terms [33].

Thus, the oscillatory dynamics are controlled by the spectral filtering term and the preservation of the soliton structure is ensured by the balance between the dispersion terms and the nonlinear terms. We have shown how the third- and fourth-order dispersion terms can destabilize the soliton structure by changing its direction and shape. This destabilization can be re-established by playing on the imaginary parts of the nonlinear gradient terms because its real parts participate in the stabilization of the structure. It is clear that in such systems the structure of the soliton can be preserved if the appropriate gains corresponding to the linear and nonlinear losses are used.

The energy exchanges take their explanation in the formula:

$$\epsilon(z) = \int_{-\infty}^{+\infty} |E(z, t)|^2 dt \quad (24)$$

with,

$$Q(z) = \frac{\epsilon(z)}{\epsilon(0)} = \frac{\eta(z)}{\eta(0)}. \quad (25)$$

$Q(z)$ is the normalization of energy, $\epsilon(z)$ is the energy of the structure and $\eta(z)$ its amplitude. We find that the normalization of energy is proportional to amplitude, which means that the normalization of energy and amplitude behave in the same way. Thus during spatial evolution, the normalization of the energy of the structure oscillates around an average value (preservation of the structure). Figures 9, 10, 11 and 12 plotted from Eq. (1) confirm this analytically determined result. Figure 11 shows that the gains made in the structure try to compensate for and exceed the losses. Figure 12 shows that the energy at any z position is about 65% of the initial energy. We will say that the soliton, to propagate lost about 35% of its initial energy. This is due to the value that the nonlinear gradient terms can take.

The system therefore has three major advantages, namely:

- The control of the spectral width ensured by the spectral filtering term β . In fact as β increases (or

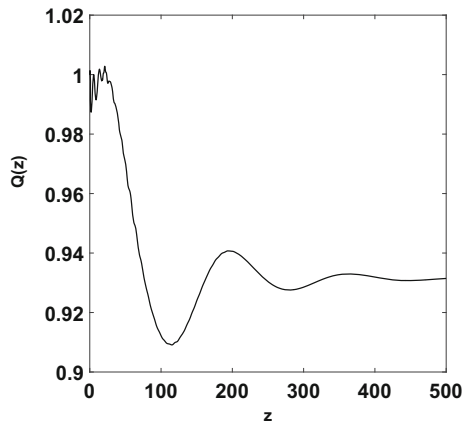


Fig. 9 Spatial evolution of the normalization of soliton energy by Eq. (1) with the parameters $\mu = -0.01, \nu = 0.43, \delta = -0.02, A = 1.43, B = 1.82, \Delta = -0.008, d = -4.25, \beta = 0.01, \beta_3 = 0.02, \beta_4 = 0.01, q_{2i} = -0.01, q_{4i} = -0.58527, q_{3i} = -0.3, q_{2r} = 0.0101, q_{3r} = -0.0125, q_{4r} = -0.0051, \varepsilon = \varepsilon_0 = 0.05219006491, \omega_{0,1} = -0.7643127702, \eta_{0,1} = 1.382310358$

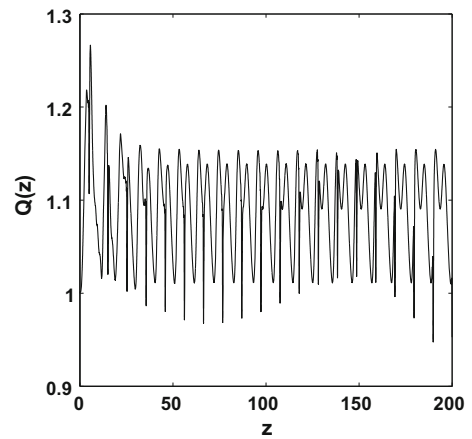


Fig. 11 Spatial evolution of the normalization of soliton energy by Eq. (1) with the parameters $\varepsilon = 0.1, \nu = 0, \mu = -0.01, \delta = -0.02, A = 2.83, B = 1.79, \Delta = -0.33, d = 15.78, \beta = 0.01, \beta_3 = 0, \beta_4 = 0.01, q_{2i} = q_{4i} = 0, q_{3i} = -0.3, q_{3r} = 0.02381, q_{4r} = -0.0051, q_{2r} = q_{2r0} = -0.0062794, \omega_0 = 3.871198193, \eta_0 = 2.310767038$

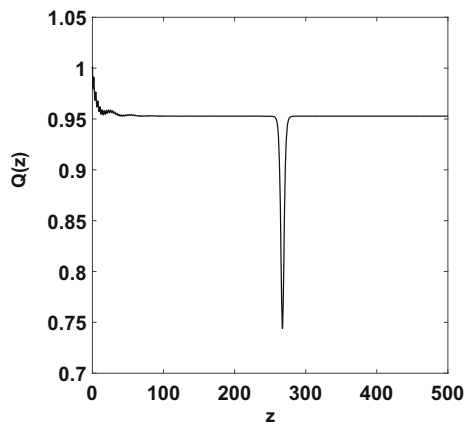


Fig. 10 Spatial evolution of the normalization of soliton energy by Eq. (1) with the parameters $\varepsilon = 0.05, \nu = 0, \delta = -0.02, A = 3.65, B = 5.48, \Delta = -0.36, d = 45.59, \beta = 0.02, \beta_3 = -0.021, \beta_4 = 0, q_{2i} = q_{4i} = 0, q_{3i} = -0.3, q_{2r} = 0.0051, q_{3r} = -0.0125, q_{4r} = -0.0051, \mu = \mu_0 = -0.001307426986, \omega_{0,1} = -1.615723557, \eta_{0,1} = 2.542222301$

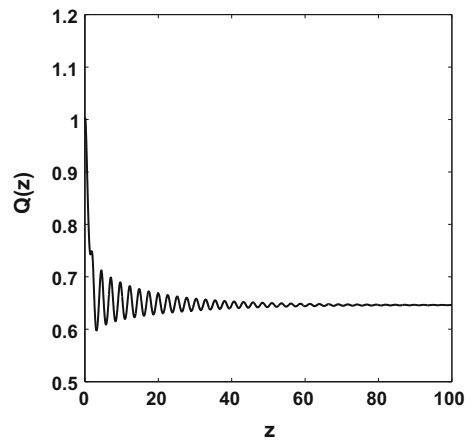


Fig. 12 Spatial evolution of the normalization of soliton energy by Eq. (1) with the parameters $\varepsilon = 0.65, \nu = 0, \mu = -0.1, \delta = -0.1, A = 1.448, B = 0.71, \Delta = -3.888, d = 10.426, \beta = 0.08, \beta_3 = -0.02, \beta_4 = 0.032, q_{2i} = 0.01, q_{3i} = 0.3, q_{4i} = 0, q_{2r} = -0.07806, q_{4r} = -0.0051, q_{3r} = q_{3r0} = 0.1980793602, \omega_{0,1} = 2.054545076$ and $\eta_{0,1} = 1.620378797$

- decreases), the oscillation frequency increases (or decreases), respectively;
- The preservation of the structure of the soliton ensured by the nonlinear gain terms $\varepsilon, \mu, q_{2r}, q_{3r}, q_{4r}$. The strong dependence of these five terms allows us to stabilize the soliton solution over very large distances;

- The change in the direction and shape of the structure provided by the dispersions terms β_3, β_4 and the nonlinear gradient terms q_{2i}, q_{3i}, q_{4i} . In addition, the fourth-order linear dispersion term (β_4) exploded the soliton profile. This explosion was compensated by the imaginary parts of the nonlinear gradient terms. Although these parameters do

not influence the stability of the fixed points, they allow us to have the soliton structure.

Thanks to these advantages, we can obtain controlled emissions over long distances with low losses and at high frequencies.

The results of our work can be applied to different dissipative systems modeled by the CCQGLE. The most promising areas where the solutions of the CCQGLE can give insight are: laser systems and optical telecommunications. Therefore, we only discuss here the use of the solutions in these areas, leaving aside other possible areas. In fact, as a physical system that is described by the CCQGLE, we can consider a soliton transmission line with linear and nonlinear gains and losses. In this case, the time-localized pulse is supported by the energy of the gains (cubic-quintic terms and nonlinear gradient terms) and the energy of the losses (spectral filtering and higher order dispersion terms). However, even a small linear loss is sufficient to destroy the stability of the pulse soliton solution. Thus, a stable stationary pulse soliton can be formed as a result of the balance between gains and losses. The ansatz (3) only works well if the higher-order dispersion is very small and the radiation tails can be neglected [13]. Moreover, the perturbation method gives satisfactory results for small values of the higher-order dispersion terms. Thus, for large values, this method is limited. However, if one wants to be interested in the large values of these terms, one must apply another perturbation method or proceed by direct numerical simulation taking as initial condition the soliton solution.

7 Conclusion

We have examined analytically and numerically the effects of nonlinear gradient terms on stationary and stable pulse solitons of the CCQGLE in the presence of spectral filtering and higher-order dispersion terms. Numerical results have shown that a small change in the value of the bifurcation parameters leads to a different behavior of the evolution of the pulse soliton solutions. The bifurcation analysis of the dynamical model proved the strong dependence of the pulse dynamics on the system parameters. The dynamical model also reveals the existence of fixed points which can be centers, saddles, sinks and sources. We have shown that it is possible to control the direction and shape of the soliton by changing the parameters that make the soliton stationary. We

also evaluated the evolution of the energy as a function of the initial energy analytically and numerically. We obtained the cases where the structure gained energy and the cases where it lost energy. To confirm the proposed dynamical model, we performed a comparison between the analytical solutions from the dynamical model and the direct numerical solutions from the basic equation. To refine our work, we propose in the near future to study the same subject by seeking the ranges of values of the system parameters for the stabilization and energy study of the structure.

Acknowledgements G. K. Saadeu acknowledges N. N. Tchepemen and R. J. Issokolo for helpful conversations. The authors would like to thank the anonymous reviewers for their useful and valuable comments and suggestions.

Data accessibility The datasets generated and analysed during the current study are available from the corresponding author on reasonable request.

Declarations

Conflicts of interest The authors declare that they have no conflict of interest concerning the publication of this manuscript.

References

1. Turing, A.: The chemical basis of morphogenesis. *Philos. Trans. R. Soc. Lond. Ser. B Biol. Sci.* **237**, 37 (1952)
2. Russell, J. S.: Report on waves, report of the fourteenth meeting of the british association for advancement of science. *Londres* **1845**, 311, Plates XLVII-LVII (1844)
3. Hasegawa, A., Tappert, F.: Transmission of stationary nonlinear optical pulses in dispersive dielectric fibers. I. Anomalous dispersion. *Appl. Phys. Lett.* **23**, 142 (1973)
4. Mollenauer, L.F., Stolen, R.H., Gordon, J.P.: Experimental observation of picoseconds pulse narrowing and solitons in optical fibers. *Phys. Rev. Lett.* **45**, 1095 (1980)
5. Hasegawa, A., Kodama, Y.: *Solitons in Optical Communications*. Clarendon, Oxford (1995)
6. Uzunov, I.M., Georgiev, Z.D., Arabadzhev, T.N.: Transitions of stationary to pulsating solutions in the Complex Cubic-Quintic Ginzburg-Landau Equation under the influence of nonlinear gain and higher-order effects. *Phys Rev E* **97**, 052215 (2018)
7. Adouane Azzedine, M.: Dynamic study of a laser associated with a complex optical system, spatial optics and precision mechanics, under the direction of M. Djabi Smail, UNIVERSITY FERHAT ABBAS - SETIF **1**, 1–134 (2019)
8. Agrawal, G.P.: *Nonlinear Fiber Optics*, 3rd edn. Academic Press, San Diego (2001)
9. Pocholle, J.P., Papuchon, M., Raffy, J., Puech, C.: Nonlinear effects in optical fibers. *Phys. Appl.* **21**, 10 (1986)

10. Latas, S.C.V.: High-Energy plain and composite pulses in a laser modeled by the complex Swift-Hohenberg equation. No. 2. *Photon. Res.* **4**, 49 (2016)
11. Afanasjev, V.V.: Interpretation of the effect of reduction of soliton interaction by bandwidth-limited amplification. *Opt. Lett.* **18**(10), 790 (1993)
12. Wang, L., Luan, Z., Zhou, Q., Biswas, A., Alzahrani, A.K., Liu, W.: Effects of dispersion terms on optical soliton propagation in a lossy fiber system. *Nonlinear Dyn.* **104**, 629–637 (2021)
13. Gurevich, S.V., Schelte, C., Javaloyes, J.: Impact of high-order effects on soliton explosions in the complex cubic-quintic Ginzburg-Landau equation. *Phys. Rev. A* **99**, 06183 (2019)
14. Chen, J., Luan, Z., Zhou, Q., Alzahrani, A.K., Biswas, A., Liu, W.: Periodic soliton interactions for higher-order nonlinear Schrödinger equation in optical fibers. *Nonlinear Dyn.* **100**, 2817–2821 (2020)
15. Akhmediev, N.N., Afanasjev, V.V., Soto-Crespo, J.M.: Singularities and special soliton solutions of the cubic-quintic complex Ginzburg-Landau equation. *Phys. Rev. E* **53**, 1190 (1996)
16. Goncalvès da Silva, E.: *Numerical Methods and Analysis*. Engineering school. Grenoble Polytechnic Institute, pp. 99. Cel-00556967 (2007)
17. Uzunov, I.M., Georgiev, ZhD, Arabadzhiev, T.N.: Influence of intrapulse Raman scattering on stationary pulses in the presence of linear and nonlinear gain as well as spectral filtering. *Phys. Rev. E* **90**, 042906 (2014)
18. Tafo, J.B.G., Nana, L.: Conrad Bertrand Tabi, Timoléon Crépin Kofané: nonlinear dynamical regimes and control of turbulence through the complex Ginzburg-Landau equation. *Intech Open.* **88053**, 18 (2020)
19. Tian, H.P., Li, Z.H., Tian, J.P., Zhou, G.S.: Effect of nonlinear gradient terms on pulsating, erupting and creeping solitons. *Appl. Phys. B* **78**, 199–204 (2004)
20. Kodama, Y., Romagnoli, M., Wabnitz, S.: Solitons in optical communications. *Electron. Lett.* **28**, 1981 (1992)
21. Moores, J.D.: On the Ginzburg-Landau laser mode-locking model with fifth-order saturable absorber term. *Opt. Commun.* **96**, 65 (1993)
22. Mollenauer, L.F., Gordon, J.P., Evangelides, S.G.: The sliding frequency guiding (an improved from soliton jitter control). *Opt. Lett.* **17**, 1575 (1992)
23. Firth, W.J., Scroggie, A.J.: Optical bullet holes (robust controllable localized states of a nonlinear cavity). *Phys. Rev. Lett.* **76**, 1623 (1996)
24. Haus, H.A., Fujimoto, J.G., Ippen, E.P.: Structures for additive pulse mode locking. *J. Opt. Soc. Am. B* **8**, 2068 (1991)
25. Ding, E., Renniger, W.H., Wise, F.W., Grelu, F., Shilizerman, E., Nathan Kutz, J.: Flower discrimination by pollinators in a dynamic chemical environment. *Int. J. Opt* **2012**, 345156 (2012)
26. Asseu, O.: Spatio-temporal pulsating dissipative solitons through collective variable methods. *J. Appl. Math. Phys. (JAMP)* **04**, 1032 (2016)
27. Drozdov, A.A., Kozlov, S.A., Sukhorukov, A.A., Kivshar, Y.S.: Self-phase modulation and frequency generation with few-cycle optical pulses in nonlinear dispersive media. *Phys. Rev. A* **86**, 053822 (2012)
28. Akhmediev, N., Afanasjev, V.V.: Novel arbitrary-amplitude soliton solutions of the cubic-quintic complex Ginzburg-Landau equation. *Phys. Rev. Lett.* **75**, 2320 (1995)
29. Van Saarloos, W., Hohenberg, P.C.: Fronts, pulses, sources and sinks in generalized complex Ginzburg-Landau equations. *Phys. D* **56**, 303 (1992)
30. Akhmediev, N.N., Ankiewicz, A.: *Solitons, Nonlinear Pulses and Beams*. Springer, Chapman and Hall, London (1997)
31. Wiggins, S.: *Introduction to Applied Nonlinear Dynamical Systems and Chaos*, 2nd edn. Springer, New York (2003)
32. Muhunthan, B., Alhattamleh, O., Zbib, H.M.: *Modeling of Localization in Granular Materials, Effect of Porosity and Particle Size*. Washington State University, Pullman, USA (2003)
33. Akhmediev, N. N., Ankiewicz, A.: In *Dissipative Solitons, Lecture Notes in Physics Vol. 661*, N. N. Akhmediev, N.N., Ankiewicz, A. (eds.). Springer, Berlin (2005)

Publisher's Note Springer Nature remains neutral with regard to jurisdictional claims in published maps and institutional affiliations.